

Synergistic catalysis by Brønsted acid and Pd species on mesoporous ZSM-5 zeolite for the oxidative homocoupling of terminal alkynes

Siming Wang,[‡] Xueqin Jia,[‡] Yongqi Sun, Jiteng Liu, Lei Zhang, Wenqian Fu* and Tiandi Tang*

School of Petrochemical Engineering, Changzhou University, Changzhou, Jiangsu 213164, P. R. China.

[‡]S.W. and X.J. contributed equally to this paper.

E-mail address: fuwenqian@cczu.edu.cn, tangtiandi@cczu.edu.cn.

1 Figures

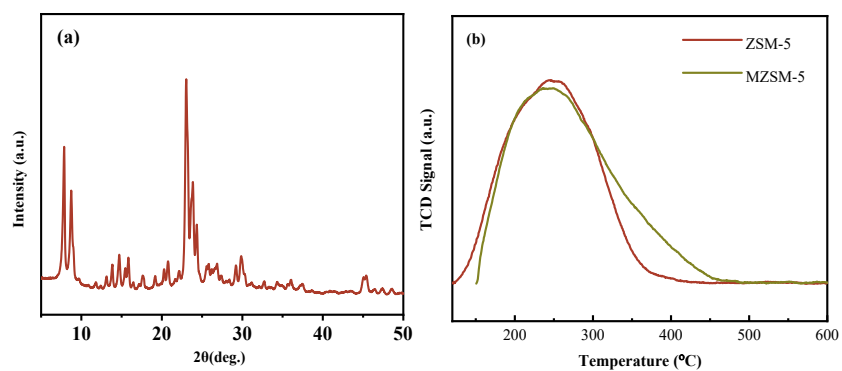


Fig. S1 (a) XRD patterns of ZSM-5, and (b) NH₃-TPD curves of ZSM-5 and MZSM-5 samples.

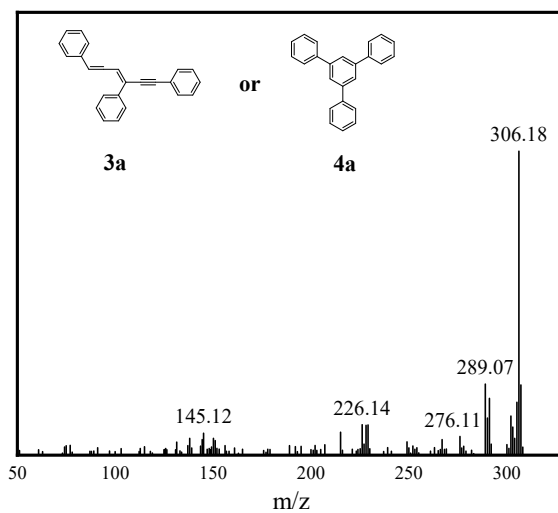


Fig. S2 GC-MS chromatogram of **3a** or **4a**.

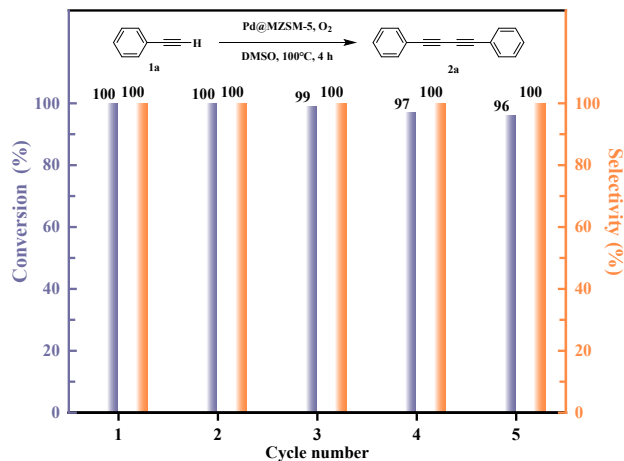


Fig. S3. Recyclability of Pd@MZSM-5 zeolite in phenylacetylene coupling reaction (Reaction conditions: 0.3 mmol **1a**, 1 mL DMSO, 30 mg Pd@MZSM-5, O₂, 4 h, 100 °C).

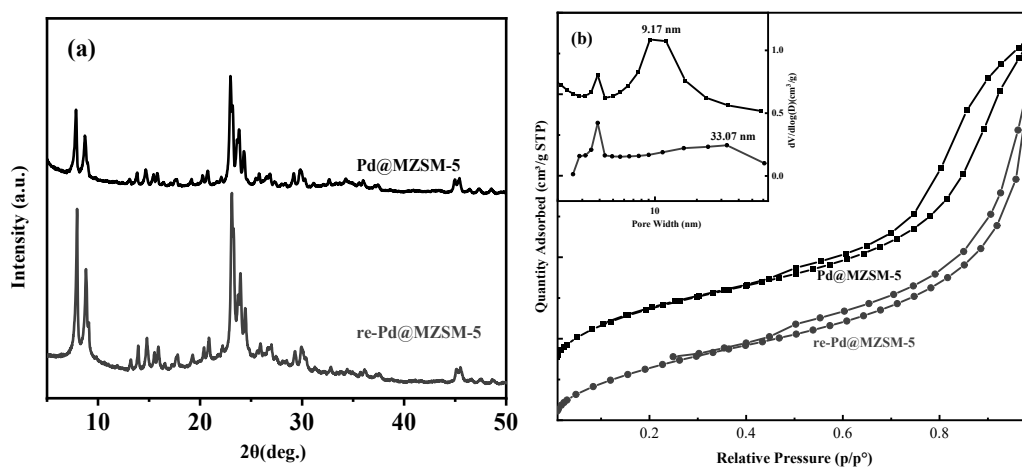


Fig. S4 (a) XRD patterns, (b) N₂ adsorption-desorption isotherm of Pd@MZSM-5 and spent Pd@MZSM-5 (referred to as re-Pd@MZSM-5) (the pore size distribution, inset).

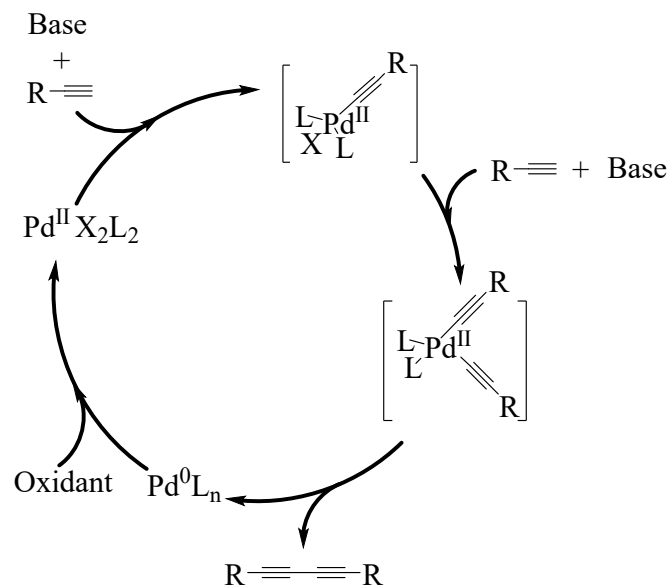


Fig. S5 Proposed General Mechanism for Pd-Catalyzed Homocoupling of Alkyne.^{S1}

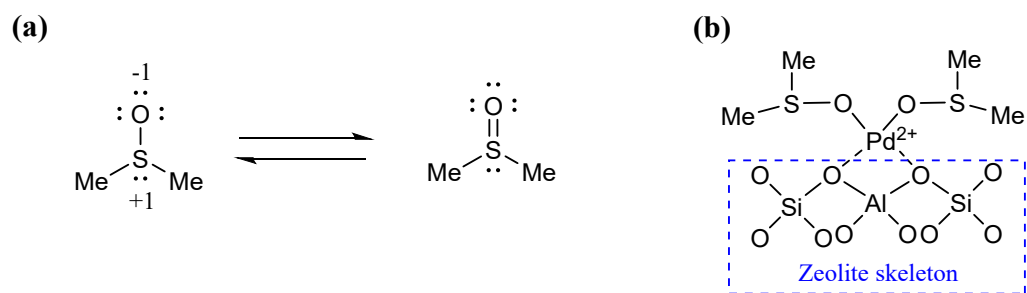


Fig. 6 Resonance structures of (a) DMSO and (b) Pd^{2+} species on zeolites bind to DMSO.

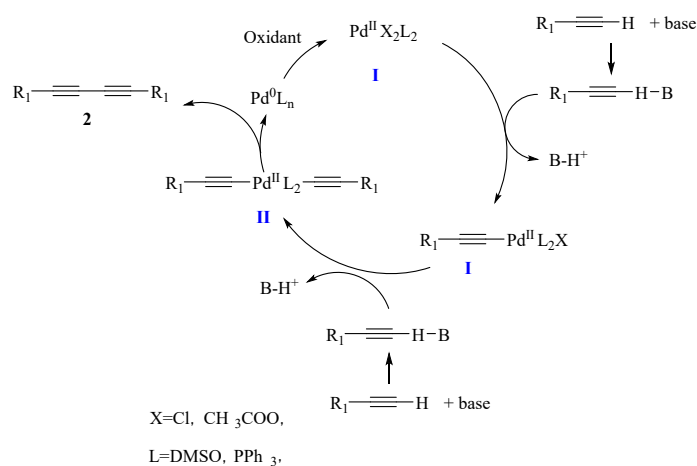


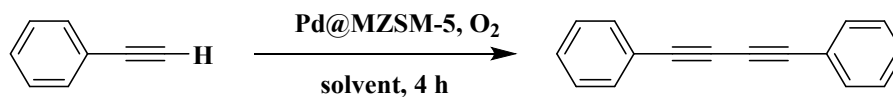
Fig. S7. The general mechanism proposed by research workers in the oxidative homocoupling reaction catalyzed by Pd-based catalyst.

Discussion:

The Glaser coupling reaction, a classical oxidative homocoupling process, was commonly employed for the synthesis of 1,3-diynes, using terminal alkynes as the starting material. Various Pd-catalyzed Glaser coupling reactions were developed, and a widely accepted and unanimous reaction mechanism was proposed^[S1-8], as shown in Fig. S7. The H atom of terminal C-H bond in the alkyne was deprotonated by the inorganic or organic bases, leading to the formation of an alkyne anion that was bonded to Pd-based catalyst to form an intermediate **I**. Another alkyne anion attacked the intermediate **I** to form Intermediate **II**, which was underwent a reductive elimination process to generate a cross-coupling product **2** and accompanied by the formation of Pd⁰L₂ complex. Pd⁰L₂ complex was re-oxidized by the oxidant form Pd²⁺X₂L₂.

2 Tables

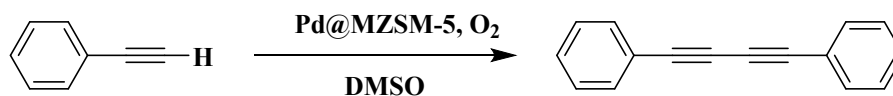
Table S1 Screening of different solvent for the oxidative homocoupling of terminal alkynes.^a



Entry	Catalyst	Solvent	Conversion ^b (%)	Selectivity ^b (%)
1	Pd@MZSM-5	N,N-Dimethylformamide	5	100
2	Pd@MZSM-5	Isopropyl alcohol	-	-
3	Pd@MZSM-5	1,4-dioxane	-	-
4	Pd@MZSM-5	Cyclohexane	-	-
5	Pd@MZSM-5	ethylbenzene	44.8	-
6	Pd@MZSM-5	Tetrahydrofuran	80	-
7	Pd@MZSM-5	1,2-Dichloroethane	23	-
8	Pd@MZSM-5	DMSO	100	100

^aReaction conditions: phenylacetylene: 0.3 mmol, 30 mg catalyst, 1 mL solvent, O₂, 4 h, 100 °C. ^bThe conversion and selectivity of the reaction were analyzed by GC.

Table S2 Screening of different temperature and time for the oxidative homocoupling of terminal alkynes.^a

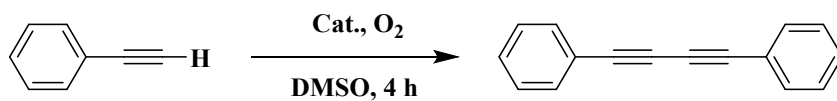


Entry	Catalyst	Temperature (°C)	Time (h)	Conversion ^b (%)	Selectivity ^b (%)
1	Pd@MZSM-5	110	4	100	100
2	Pd@MZSM-5	100	4	100	100
3	Pd@MZSM-5	90	4	89	100
4	Pd@MZSM-5	80	4	63	100
5	Pd@MZSM-5	100	1	72	100
6	Pd@MZSM-5	100	1.5	84	100
7	Pd@MZSM-5	100	2.5	100	100

^aReaction conditions: phenylacetylene: 0.3 mmol, 30 mg catalyst, 1 mL DMSO, O₂.

^bThe conversion and selectivity of the reaction were analyzed by GC.

Table S3 Screening of different metal loading for the oxidative homocoupling of terminal alkynes. ^a



Entry	Catalyst	Atmosphere	Time (h)	Conversion ^b (%)	Selectivity ^b (%)
1	1% Pd@MZSM-5	O ₂	4	100	100
2	2% Pd@MZSM-5	O ₂	4	100	100
3	4% Pd@MZSM-5	O ₂	4	100	96
4	8% Pd@MZSM-5	O ₂	4	100	78

Reaction conditions: phenylacetylene: 0.3 mmol, 30 mg Pd@MZSM-5, 1 mL DMSO, O₂, 4 h, 100 °C. ^bThe conversion and selectivity of the reaction were analyzed by GC.

Table S4 Oxidative homocoupling of terminal alkynes reaction in the published works.

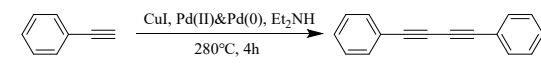
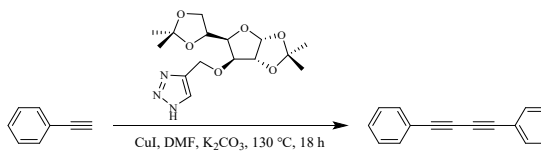
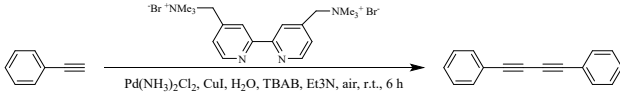
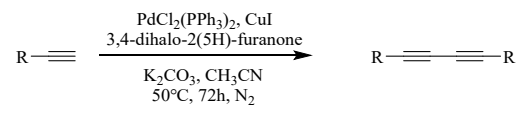
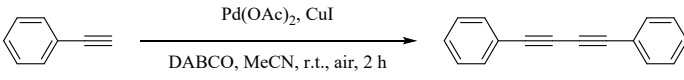
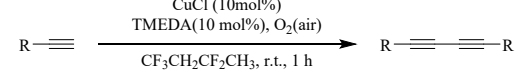
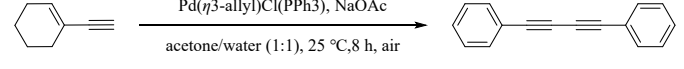
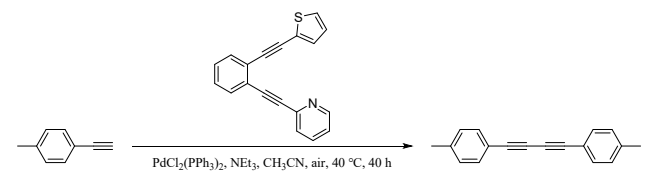
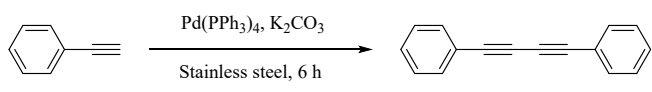
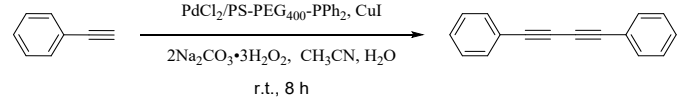
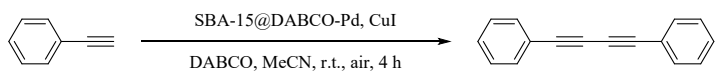
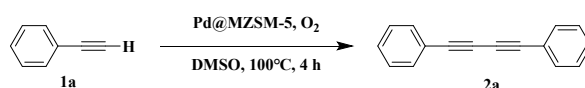
Entry	Reaction condition	Yield (%)	Reference
1		63	S4
2		38-99	S9
3		44-94	S10
4		76~90	S11
7		100	S12
5		82~98	S13
6		83	S1
8		67	S3
9		74	S14
10		96	S15
11		100	S16

Table S5 Textural parameter characteristics of the materials.

Catalysts	S_{BET}^a ($\text{m}^2 \cdot \text{g}^{-1}$)	$S_{\text{meso.}}^b$ ($\text{m}^2 \cdot \text{g}^{-1}$)	$V_{\text{micro.}}^c$ ($\text{cm}^3 \cdot \text{g}^{-1}$)	$V_{\text{meso.}}^d$ ($\text{cm}^3 \cdot \text{g}^{-1}$)
Pd@MZSM-5	428	219	0.09	0.37
Spent Pd@MZSM-5	405	205	0.09	0.39

^a BET surface area. ^b External surface area. ^c Microporous volume. ^d Mesoporous volume.

Table S6 Influence of different catalysts on the activity of phenylacetylene coupling reaction ^a

Entry	Catalyst	Time (h)	Conversion (%)	Selectivity (%)
1	Pd@MZSM-5	4	100	100
2	Pd@MZSM-5-R	4	34	100
3 ^c	Pd@MZSM-5-E	4	83	100
4 ^d	Pd@MZSM-5-C	4	-	-

^aReaction conditions: 0.3 mmol phenylacetylene, 30 mg catalyst, 1 mL DMSO, 100 °C, 4 h, O₂. ^b The catalyst was flowed with H₂ and reduced at 450 °C, after cooling to room temperature, it was passivated with general N₂/O₂ mixture gas for 1 h. ^c The catalyst was prepared by ion exchange. ^d The catalyst was calcined at 450 °C.

Discussion:

To explore whether an optimal ratio between the Pd⁰ and Pd²⁺ species was present or not, a series of Pd@MZSM-5 catalysts with different Pd states were prepared and subjected to activity testing. The Pd@MZSM-5 catalyst was calcined at 450 °C, which was denoted as Pd@MZSM-5-C. The Pd@MZSM-5 catalyst was directly reduced at 450 °C in H₂ stream, and the reduced catalyst was named as

Pd@MZSM-5-R.

The activity data in Table S6 showed that compared with Pd@MZSM-5 catalyst, Pd@MZSM-5-R catalyst was poor activity, giving conversion of 34% (entries 1 and 2). Pd@MZSM-5-E catalyst showed moderate activity, giving 83% conversion (entry 3). It is strange that the Pd@MZSM-5-C catalyst was inactivity for this reaction (entry 4). These activity data suggested that the electronic state of the Pd species in the catalyst played an important role in enhancing the reaction activity, considering these catalysts had similar textural parameters (Table S7). The Pd@MZSM-5-R catalyst should have a larger percentage of Pd⁰ than Pd@MZSM-5 catalyst, nevertheless, the activity of Pd@MZSM-5-R was lower than that of Pd@MZSM-5 catalyst. These results implied that the role of Pd²⁺ in the reaction is more pronounced than that of Pd⁰, which could be because in the initial reaction stage, the Pd²⁺ species was preferential coordinated with the absorbed phenylacetylene to form a alkynyl-palladium(II) complex, leading to the reaction further proceeding. In the case for Pd@MZSM-5-R, although partial of Pd⁰ can be oxidize to Pd²⁺ under O₂ atmosphere, the low percentage of Pd²⁺ led to low activity of the Pd@MZSM-5-R catalyst.

The inactivity of the Pd@MZSM-5 catalyst could be due to the fact that majority of Pd species should be present in the form of PdO species after high-temperature calcination, and the PdO was not the active site. This was because the oxygen atom in the PdO phase strongly interacted with Pd atoms, inhibiting the Pd atom coordination with the substrate and DMSO molecule.

The relatively low activity of Pd@MZSM-5-E catalyst was attributed to the low proportion of Pd⁰ (23%), from the XPS spectra of the Pd@MZSM-5-E and Pd@MZSM-5 catalysts (Fig. 3a). In the Pd-catalyzed oxidative homocoupling of terminal alkynes, active Pd²⁺ and Pd⁰ species were required to be reversibly transformed under reaction condition. The relatively low Pd⁰ content on Pd@MZSM-5-E catalyst may go against the reversible transformation.

As discussion above, although Pd⁰ and Pd²⁺ are beneficial to the reaction, the contribution of Pd²⁺ to the reaction is more significant than that of Pd⁰. In addition,

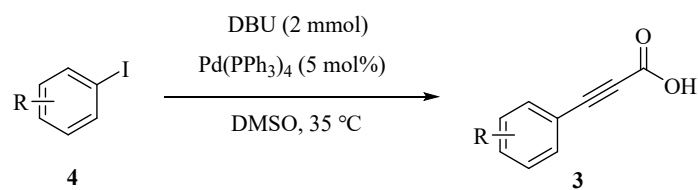
the relatively low Pd⁰ content on catalyst may go against the reversible transformation between Pd²⁺ and Pd⁰ species. Therefore, the ratio of Pd²⁺/Pd⁰ (1.6) on Pd@MZSM-5 was appropriate for this reaction.

Table S7 Textural parameters of the materials.

Catalysts	S _{BET} (m ² /g) ^a	S _{ext.} (m ² /g) ^b	V _{micro.} (cm ³ /g) ^c	V _{meso.} (cm ³ /g) ^d
Pd@MZSM-5	428	219	0.09	0.37
Pd@MZSM-5-R	392	214	0.09	0.22
Pd@MZSM-5-E	414	213	0.09	0.37
Pd@MZSM-5-C	413	216	0.09	0.31

^aBET surface area. ^bExternal surface area. ^cMicroporous volume. ^dMesoporous volume.

Table S8 Synthesis of acetylenic acid substrates.^a

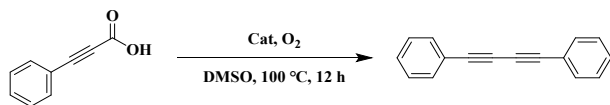


Substrate	Product	Conversion ^b (%)	Selectivity ^b (%)
	 3b	55	99
	 3c	62	95
	 3d	69	92
	 3f	60	99
	 3l	65	93

^aReaction conditions: a 100 mL round-bottom flask was charged with tetrakis(triphenylphosphine)palladium ($\text{Pd(PPh}_3)_4$) (5 mol%), iodobenzene (1.0 mmol), 2,3,4,6,7,8,9,10-octahydropyrimido[1,2-a]azepine (DBU)(2 mmol), and 5 mL of DMSO. A solution of acetylenic acid (1.1 mmol) in DMSO (5 mL) was then added dropwise. The reaction mixture was heated in an oil bath at 35 °C for 10 h, after which it was cooled to room temperature. The reaction mixture was then diluted with ethyl acetate and extracted with a saturated solution of sodium bicarbonate. The aqueous layer was separated, acidified to pH 2.0 with dilute hydrochloric acid, and extracted with dichloromethane. The combined organic layers were dried over anhydrous sodium sulfate, filtered, and the solvent was removed under reduced pressure using a

rotary evaporator. The crude product was purified by silica gel column chromatography to yield the acetylenic acid product. By changing the substituents on the iodobenzene substrate, acetylenic acid products with different substituents were synthesized.^{S17} ^bThe conversion and selectivity of the reaction were analyzed by GC.

Table S9 Screening of different catalysts for the decarboxylation coupling of phenylpropargylic acid.^a

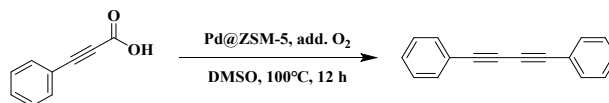


Entry	Catalyst	Additive	Conversion ^b	Selectivity ^b
			(%)	(%)
1	-	-	-	-
2	PdCl ₂ ^c	-	100	-
3	Pd(NO ₃) ₂ ^c	-	100	-
4	Pd(OAc) ₂ ^c	-	100	-
5	Pd@MZSM-5	-	100	74
6	Pd@MSilicalite-1	-	30	27

^aReaction conditions: 0.3 mmol phenylpropargylic acid, 30mg catalyst, 1 mL DMSO, O₂, 12 h, 100 °C. ^bThe conversion and selectivity of the reaction were analyzed by GC.

^c0.03 mmol (10 mol%).

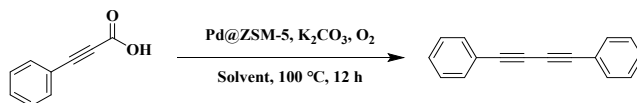
Table S10 Screening of different additives for the decarboxylation coupling of phenylpropargylic acid.^a



Entry	Catalyst	Additive	Conversion ^b	Selectivity ^b
			(%)	(%)
1	Pd@MZSM-5	-	100	74
2	Pd@MZSM-5	K ₂ CO ₃	100	100
3	Pd@MZSM-5	KI	100	83
4	Pd@MZSM-5	Cs ₂ CO ₃	100	79
6	Pd@MZSM-5	KOH	100	66

^a Reaction conditions: 0.3 mmol phenylpropargylic acid, 30mg catalyst, 1 mL DMSO, 50 mg additive, O₂, 12 h, 100 °C. ^bThe conversion and selectivity of the reaction were analyzed by GC.

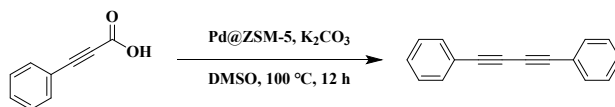
Table S11 Screening of different solvents for the decarboxylation coupling of phenylpropargylic acid.^a



Entry	Catalyst	Solvent	Conversion ^b	Selectivity ^b
			(%)	(%)
1	Pd@MZSM-5	Dimethyl sulfoxide	100	100
2	Pd@MZSM-5	Tetrahydrofuran	69	5
3	Pd@MZSM-5	N,N-Dimethylformamide	87	29
4	Pd@MZSM-5	Acetonitrile	0	0

^a Reaction conditions: 0.3 mmol phenylpropargylic acid, 30 mg catalyst, 1 mL solvent, 50 mg K₂CO₃, O₂, 12 h, 100 °C. ^bThe conversion and selectivity of the reaction were analyzed by GC.

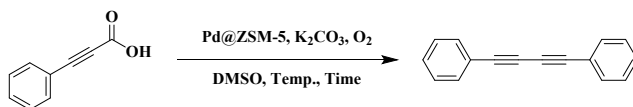
Table S12 Screening of different atmospheres for the decarboxylation coupling of phenylpropargylic acid.^a



Entry	Catalyst	Additive	Atmosphere	Conversion ^b (%)	Selectivity ^b (%)
1	Pd@MZSM-5	K ₂ CO ₃	O ₂	100	100
2	Pd@MZSM-5	K ₂ CO ₃	Air	94	76
3	Pd@MZSM-5	K ₂ CO ₃	N ₂	82	47

^a Reaction conditions: 0.3 mmol phenylpropargylic acid, 30 mg catalyst, 1 mL DMSO, 50 mg K₂CO₃, 12 h, 100 °C. ^bThe conversion and selectivity of the reaction were analyzed by GC.

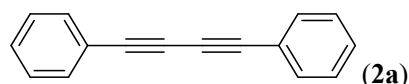
Table S13 Screening of different temperature and time for the decarboxylation coupling of phenylpropargylic acid.^a



Entry	Catalyst	Temperature (°C)	Time (h)	Conversion ^b (%)	Selectivity ^b (%)
1	Pd@MZSM-5	100	12	100	100
2	Pd@MZSM-5	90	12	100	100
3	Pd@MZSM-5	80	12	75	100
4	Pd@MZSM-5	70	12	0	0
5	Pd@MZSM-5	100	8	94	100
6	Pd@MZSM-5	100	6	67	100
7	Pd@MZSM-5	100	3	43	100

^a Reaction conditions: 0.3 mmol phenylpropargylic acid, 30 mg catalyst, 1 mL DMSO, 50 mg K₂CO₃. ^bThe conversion and selectivity of the reaction were analyzed by GC.

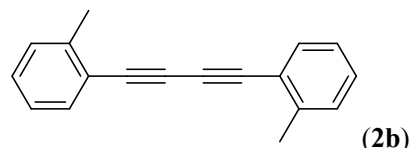
3. Characterization of the products



1,4-Diphenyl buta-1,3-diyne: white solid

¹H NMR (400 MHz, Chloroform-*d*) δ 7.46 (t, *J* = 7.9, 1.7 Hz, 4H), 7.33 – 7.24 (m, 6H).

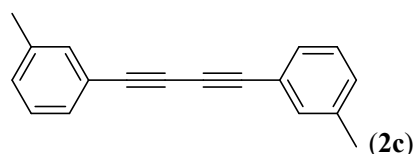
.....



1,4-di-o-tolylbuta-1,3-diyne: white solid

¹H NMR (300 MHz, Chloroform-*d*) δ 7.34 (d, *J* = 7.6 Hz, 4H), 7.27 – 7.14 (m, 5H), 2.34 (s, 6H).

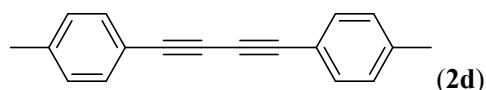
.....



1,4-di-m-tolylbuta-1,3-diyne: white solid

¹H NMR (300 MHz, Chloroform-*d*) δ 7.50 (d, *J* = 7.6 Hz, 2H), 7.32 – 7.10 (m, 6H), 2.50 (s, 6H).

.....



1,4-di-p-tolylbuta-1,3-diyne: white solid

¹H NMR (300 MHz, CDCl₃) δ 7.42 (d, *J* = 7.8 Hz, 4H), 7.14 (d, *J* = 7.8 Hz, 4H), 2.36 (s, 6H).

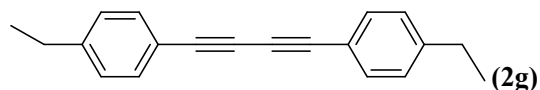
.....



Benzene, 1,1'-(1,3-butadiyne-1,4-diyl)bis[4-methoxy-: white solid

GC-MS (EI, 70 eV): *m/z* (%): 262.09(100.00), 219.08(16.81), 176.05(15.89), 131.07(7.87), 94.38(4.51).

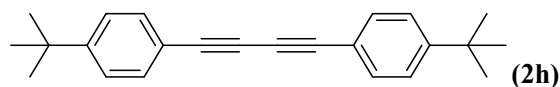
.....



1,4-bis(4-ethylphenyl)buta-1,3-diyne: white solid

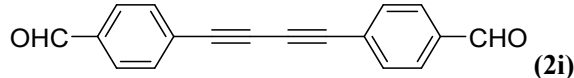
GC-MS (EI, 70 eV): *m/z* (%): 258.19(100.00), 243.17(82.13), 228.14(30.16), 114.04(13.60), 213.14(3.94).

.....



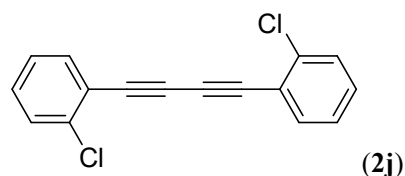
1,1'-(1,3-Butadiyne-1,4-diyl)bis[4-(1,1-dimethylethyl)benzene]: white solid

GC-MS (EI, 70 eV): m/z (%): 299.22(100.00), 314.24(65.20), 114.08(20.34), 142.12(13.68), 241.13(6.41).



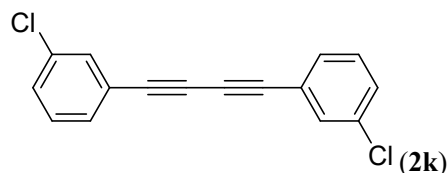
4,4'-(1,3-Butadiyne-1,4-diyl)bis[benzaldehyde]: white solid

GC-MS (EI, 70 eV): m/z (%): 258.08(100.00), 200.09(36.29), 96.02(30.93), 229.13(21.21), 74.04(9.58).



1,4-bis(2-chlorophenyl)buta-1,3-diyne: light yellow solid

¹H NMR (300 MHz, Chloroform-*d*) δ 7.58 (dd, *J* = 7.5, 2.0 Hz, 2H), 7.42 (d, *J* = 7.9 Hz, 2H), 7.35 – 7.19 (m, 6H).



1,4-bis(3-chlorophenyl)buta-1,3-diyne: white solid

¹H NMR (300 MHz, Chloroform-*d*) δ 7.51 (d, *J* = 1.9 Hz, 2H), 7.46 – 7.22 (m, 7H).



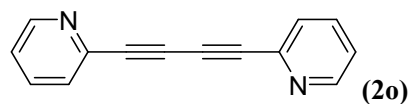
1,4-bis(4-chlorophenyl)buta-1,3-diyne: colorless solid

GC-MS (EI, 70 eV): m/z (%): 269.99(100.00), 200.05(33.11), 134.98(8.74), 100.01(7.86), 174.04(6.32).



1,4-bis(4-fluorophenyl)buta-1,3-diyne: white solid

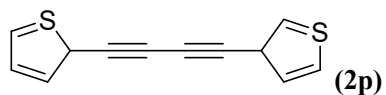
¹H NMR (300 MHz, Chloroform-*d*) δ 7.51 (dd, *J* = 8.4, 5.4 Hz, 4H), 7.04 (t, *J* = 8.5 Hz, 4H).



2,2'-(1,3-Butadiyne-1,4-diyl)bis[pyridine]: light yellow solid

GC-MS (EI, 70 eV): m/z (%): 204.11(100.00), 176.07(10.18),150.08(8.56), 99.01(6.42), 77.05(5.53).

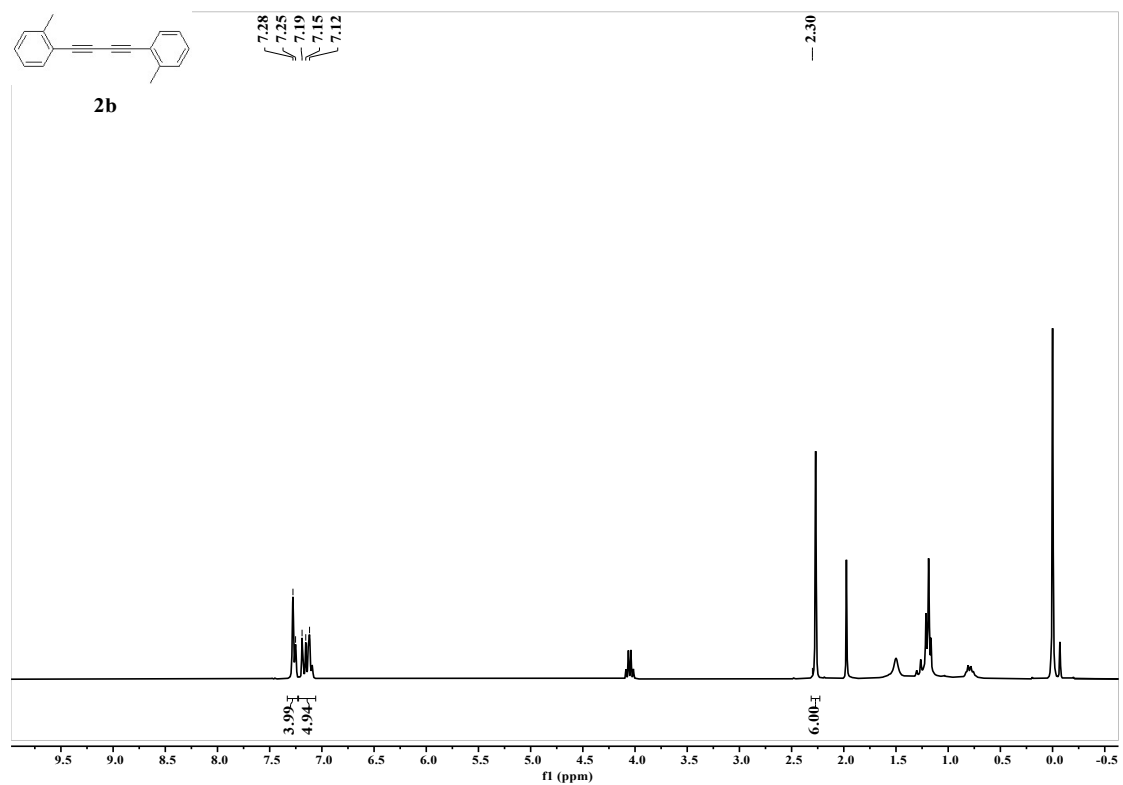
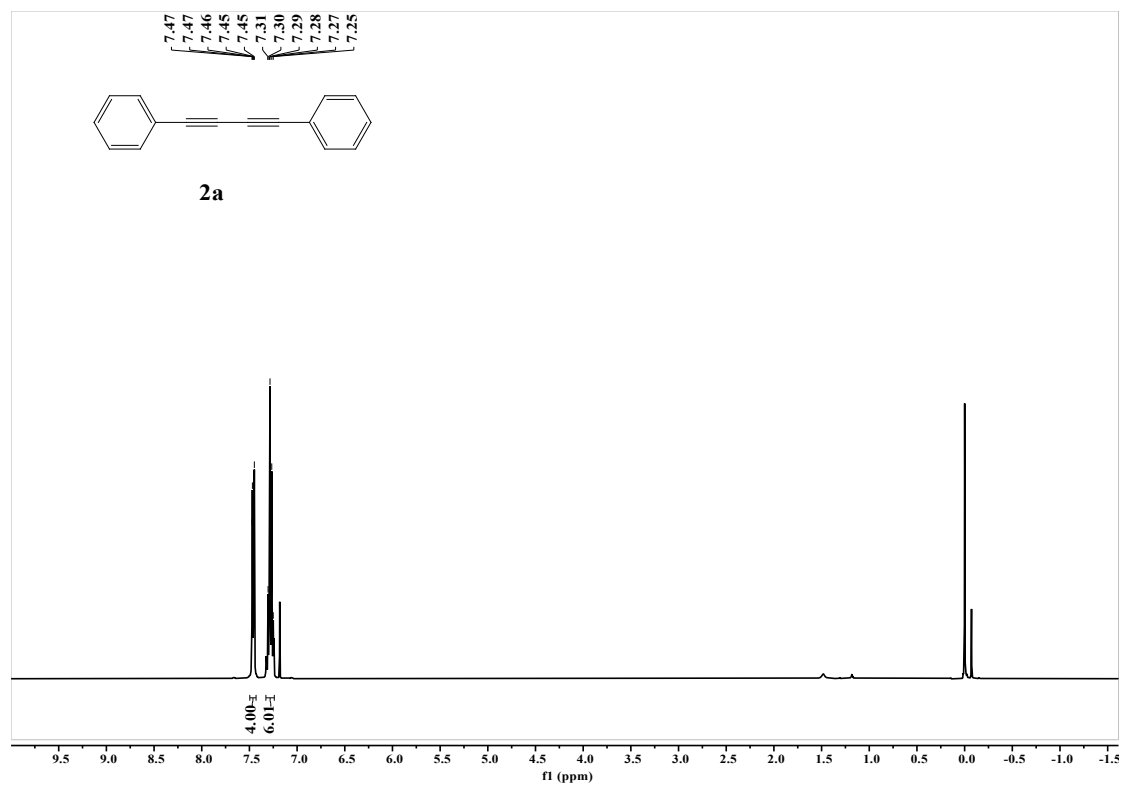
.....

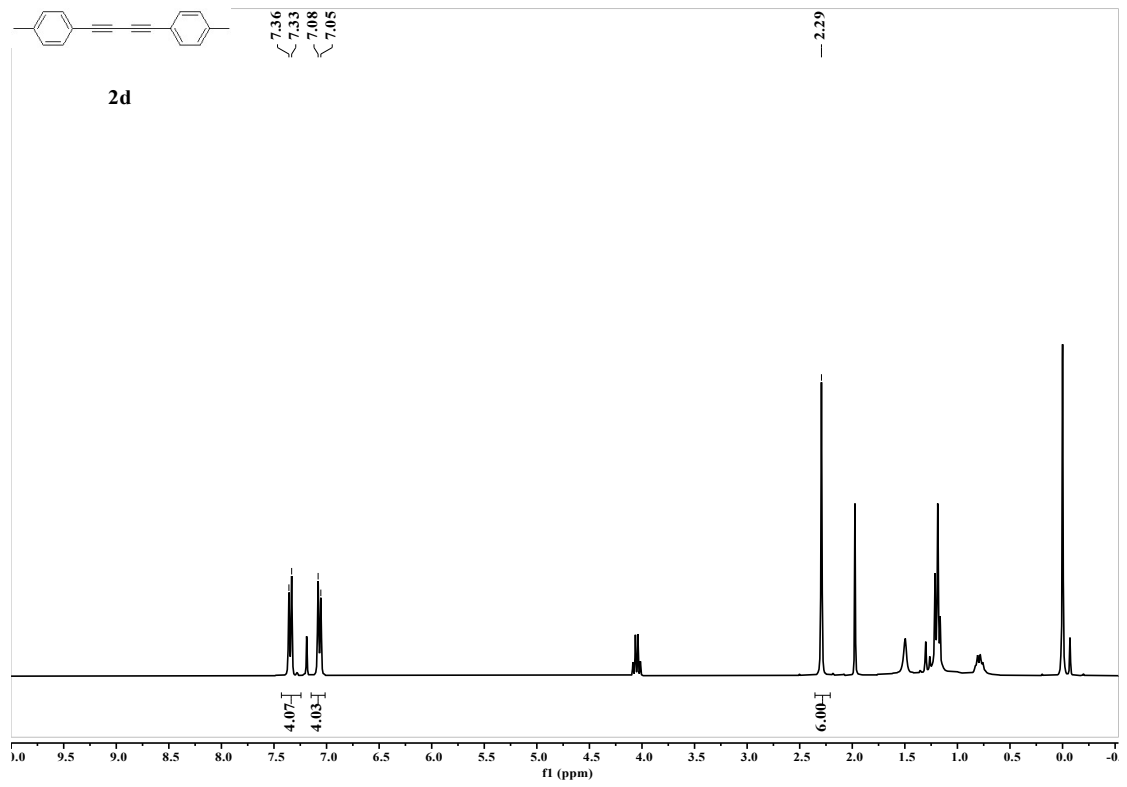
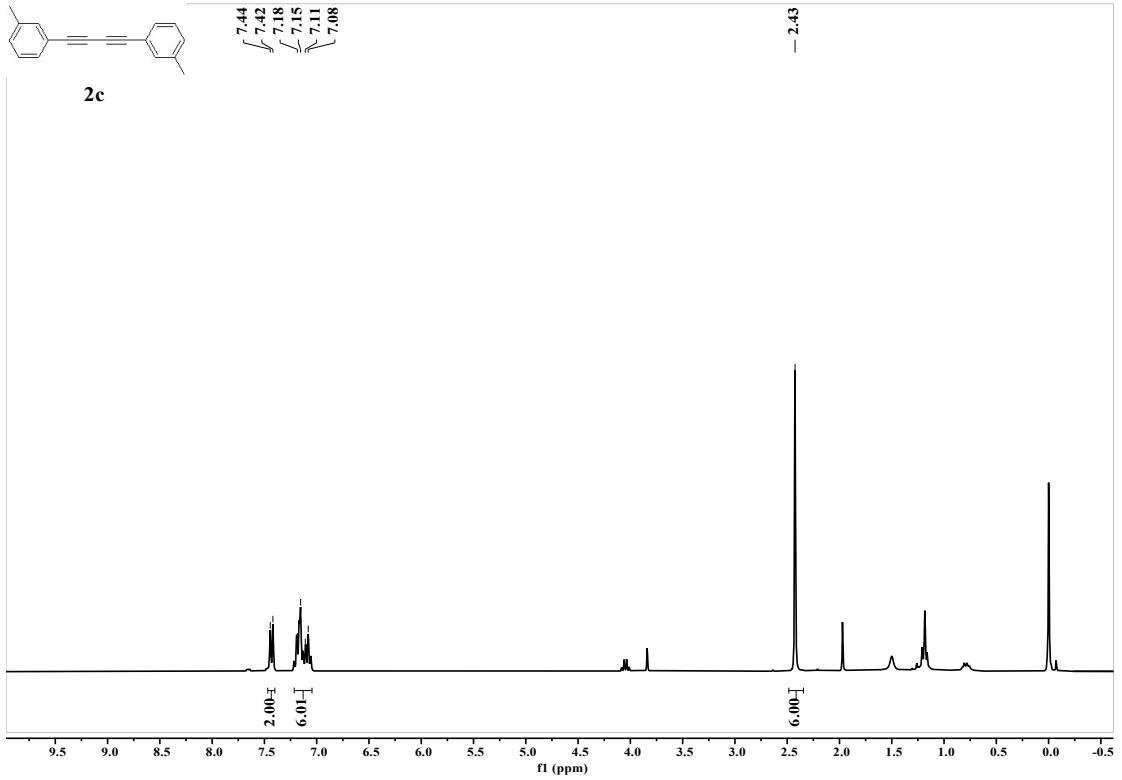


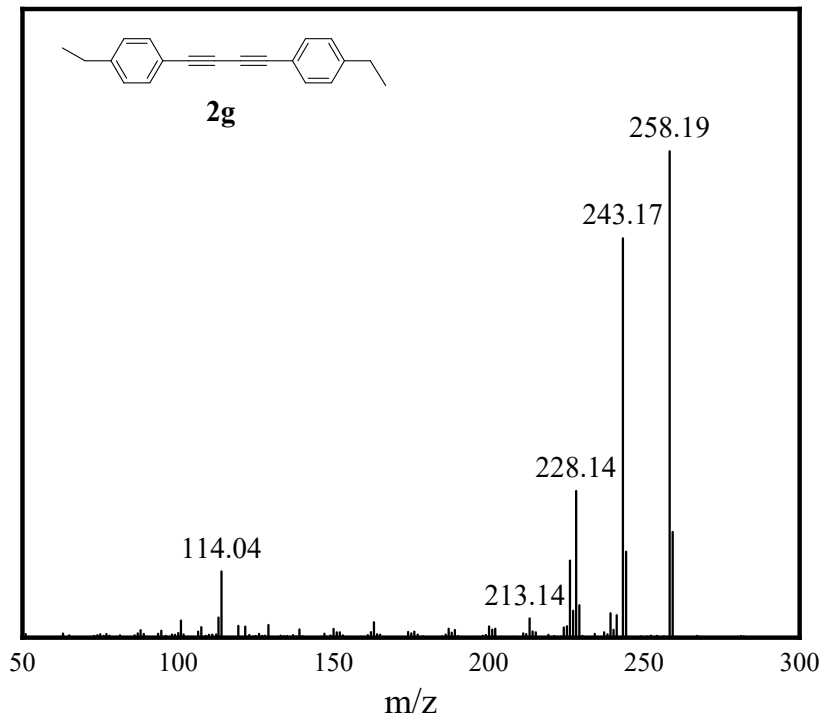
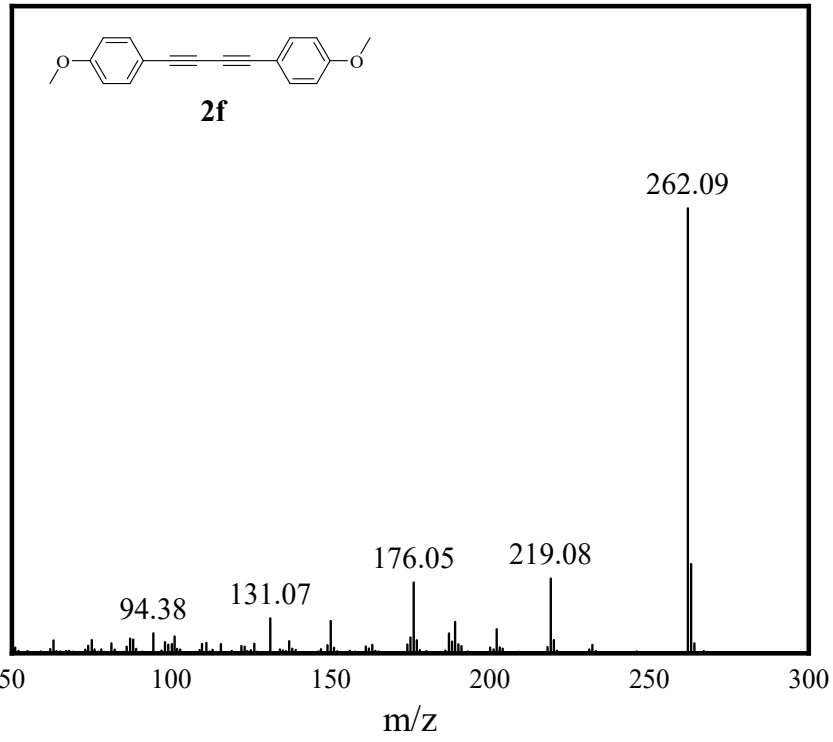
2-[4-(3-Thienyl)-1,3-butadiyn-1-yl]thiophene: light yellow solid

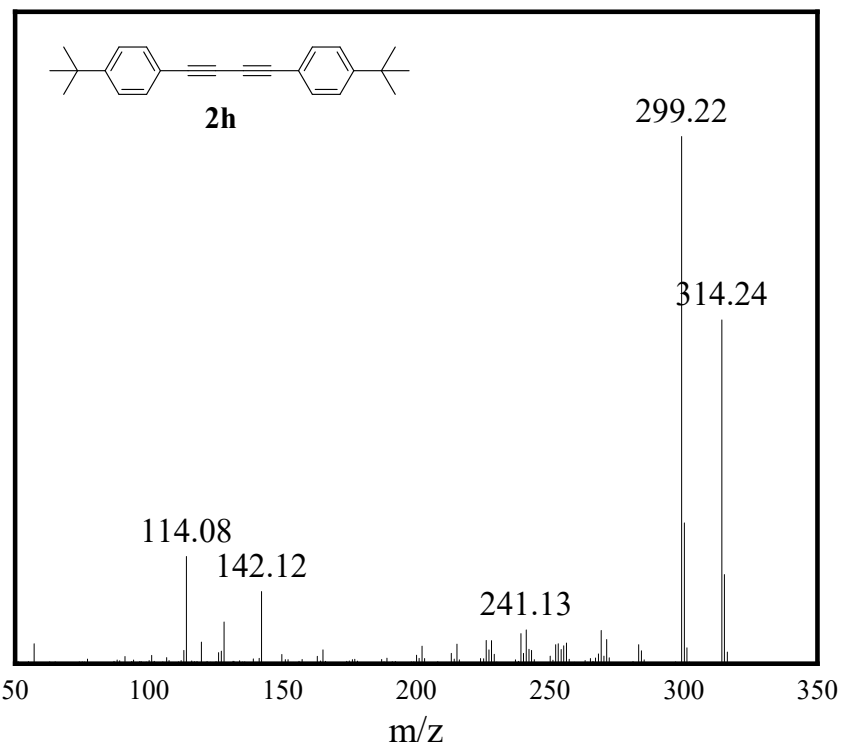
GC-MS (EI, 70 eV): m/z (%): 216.04(100.00), 171.04(28.44),184.06(6.48),139.07(5.39), 85.99(4.96).

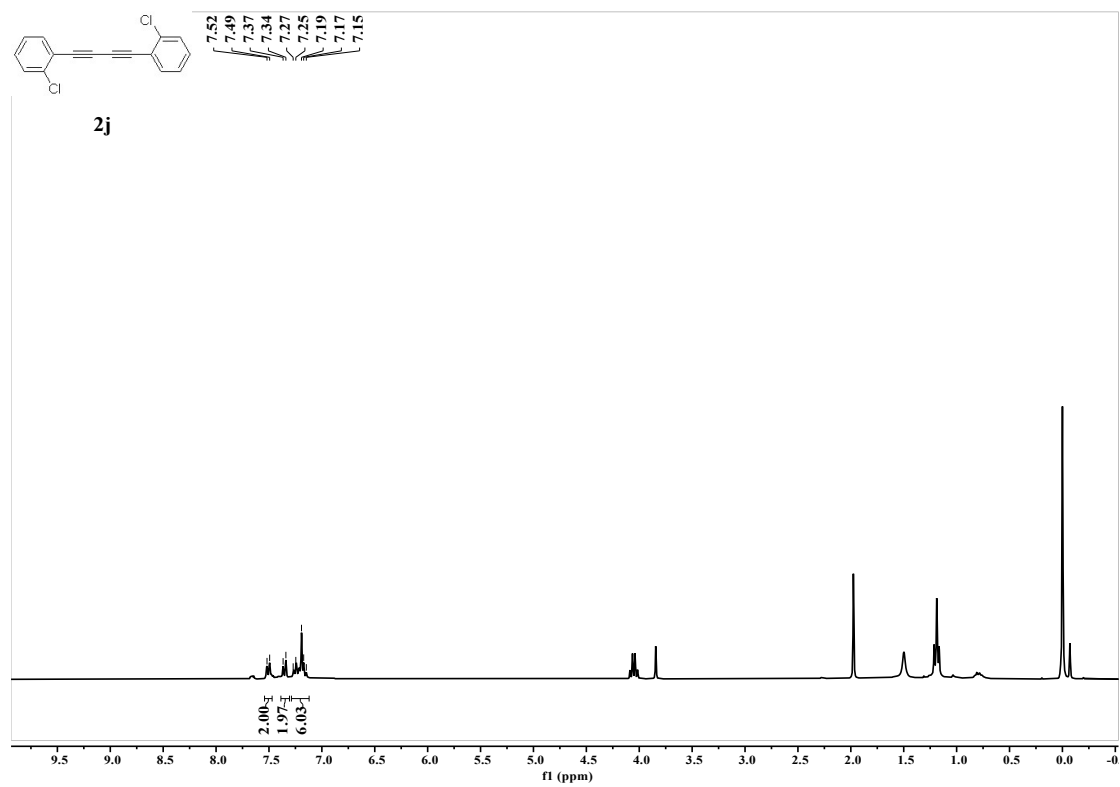
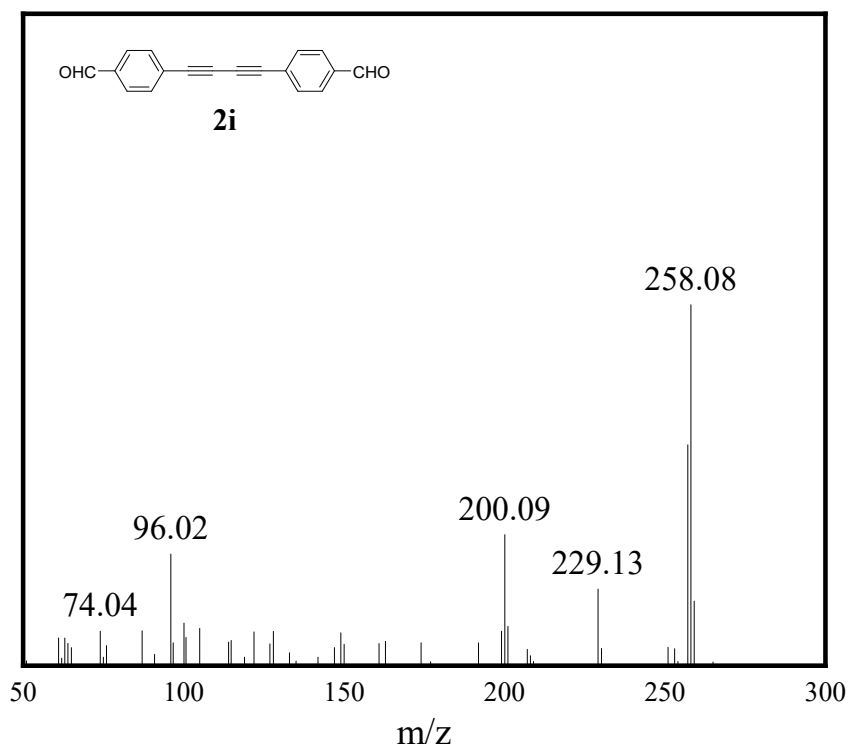
4. The spectrums of ^1H NMR and GC-MS.

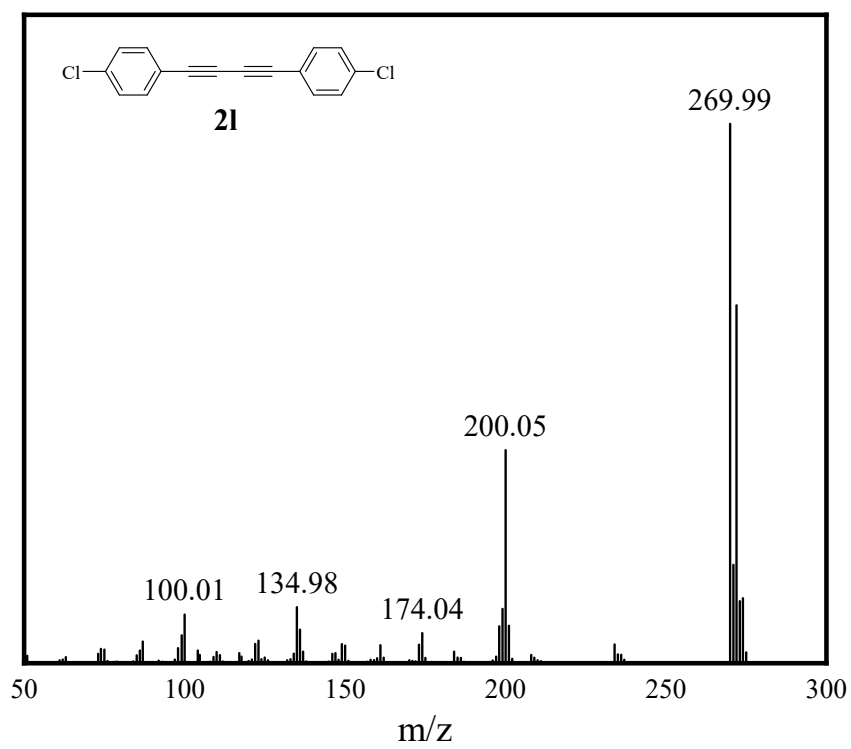
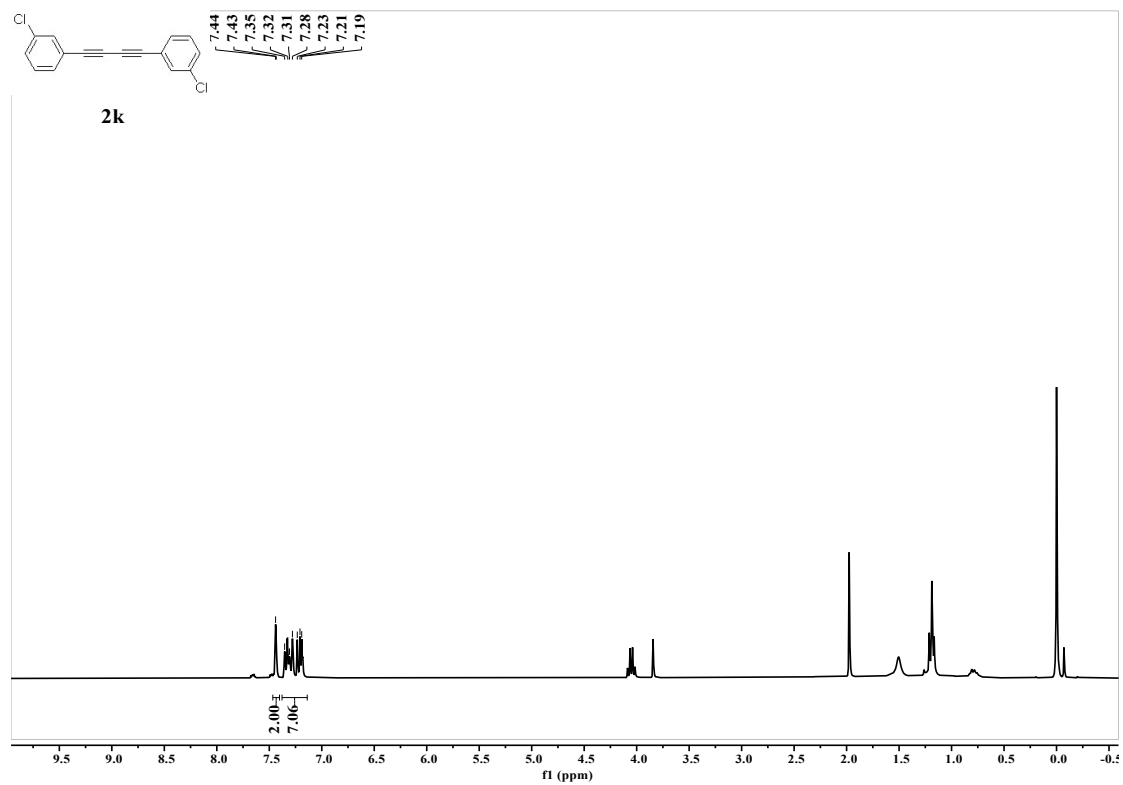


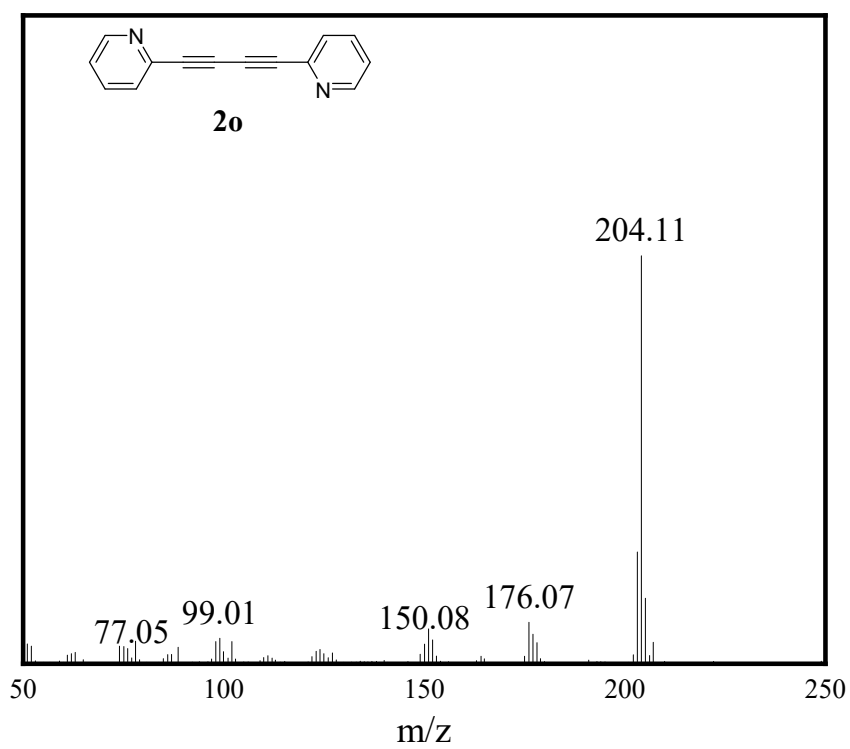
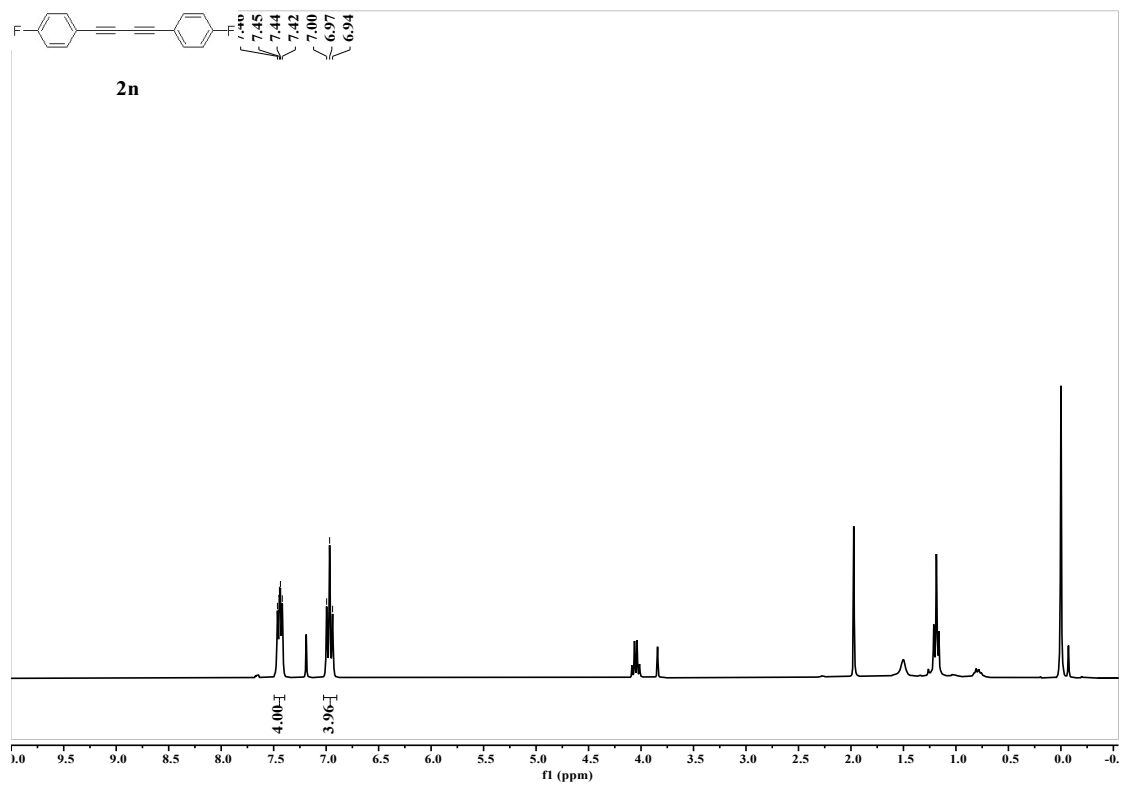


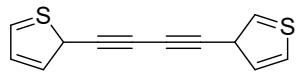




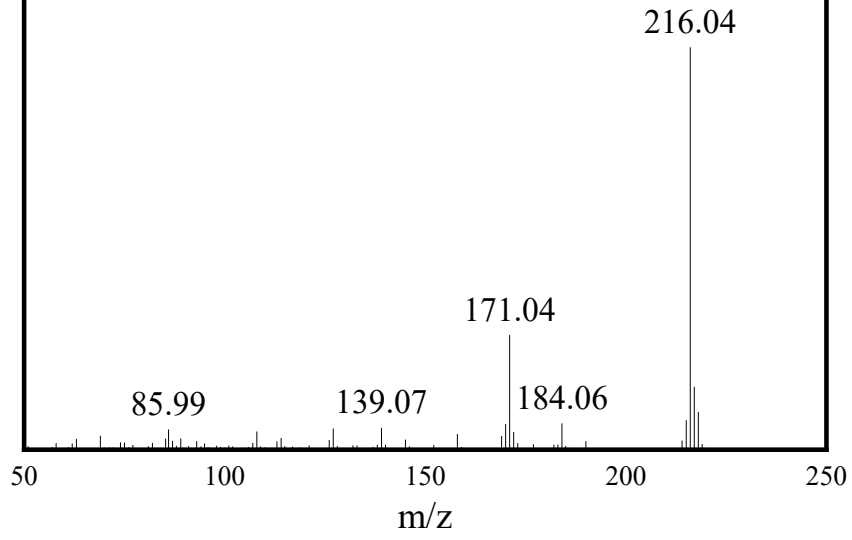








2p



5 References

- 1 A. Toledo, I. Funes-Ardoiz, F. Maseras, A.C.J.A.C. Albeniz, *ACS Catal.*, 2018, **8**, 7495-7506.
- 2 F. Alonso, M.J.A.C. Yus, *ACS Catal.*, 2012, **2**, 1441-1451.
- 3 S. Atobe, M. Sonoda, Y. Suzuki, T. Yamamoto, H. Masuno, H. Shinohara, A.J.R.o.C.I. Ogawa, *Res. Chem. Inter.*, 2013, **39**, 359-370.
- 4 M. Hattori, S.-i. Yamaura, W. Zhang, W. Sakamoto, T.J.M.L. Yogo, *Mater. Lett.*, 2021, **303**, 130498.
- 5 Z. Shi, C. Zhang, C. Tang, N.J.C.S.R. Jiao, *Chem. Soc. Rev.*, 2012, **41**, 3381-3430.
- 6 H.A. Stefani, A.S. Guarezemini, R.J.T. Cella, *Tetrahedron*, 2010, **66**, 7871-7918.
- 7 N. Sun, Y. Yun, K. Li, X. Ni, Y. Qin, X. Yang, H. Sheng, M.J.E.J.o.I.C. Zhu, *Eur. J. Inorgan. Chem.*, 2023, **26**, e202300161.
- 8 W. Zierkiewicz, T.J.O. Privalov, *Organometallics*, 2005, **24**, 6019-6028.
- 9 N. Mishra, S.K. Singh, A.S. Singh, A.K. Agrahari, V.K.J.T.J.o.O.C. Tiwari, *J. Org. Chem*, 2021, **86**, 17884-17895.
- 10 S.-N. Chen, W.-Y. Wu, F.-Y.J.G.C. Tsai, *Green Chem.*, 2009, **11**, 269-274.
- 11 J.-X. Li, H.-R. Liang, Z.-Y. Wang, J.-H.J.M.f.C.-C.M. Fu, *Monatshefte Chem.*, 2011, **142**, 507-513.
- 12 J.-H. Li, Y. Liang, Y.-X.J.T.J.o.o.c. Xie, *J. Org. Chem.*, 2005, **70**, 4393-4396.
- 13 A. Kusuda, X.-H. Xu, X. Wang, E. Tokunaga, N.J.G.C. Shibata, 2011, **13**, 843-846.
- 14 L. Chen, B.E. Lemma, J.S. Rich, J.J.G.c. Mack, *Green chem.*, 2014, **16**, 1101-1103.
- 15 L. Zhou, H.Y. Zhan, H.L. Liu, H.F.J.C.J.o.C. Jiang, *Chinese J. Chem.*, 2007, **25**, 1413-1416.
- 16 H. Li, M. Yang, Q.J.M. Pu, *Micropor. Mesopor. Mat.* 2012, **148**, 166-173.
- 17 K. Park, G. Bae, J. Moon, J. Choe, K.H. Song, S.J.T.J.o.O.C. Lee, *J. Org. Chem.*, 2010, **75**, 6244-6251.